J Mol Model (2010) 16:1093–1101
DOI 10.1007/s00894-009-0610-2

ORIGINAL PAPER

Are density functional theory predictions of the Raman spectra accurate enough to distinguish conformational transitions during amyloid formation?

Workalemahu Mikre Berhanu · Ivan A. Mikhailov · Artëm E. Masunov

Received: 11 August 2009 / Accepted: 2 October 2009 / Published online: 20 November 2009

Abstract We report density functional theory (DFT) calculations of the Raman spectra for hexapepetides of glutamic acid and lysine in three different conformations (α, β and PPII). The wave numbers of amide I, amide II and amide III bands of all three conformations predicted at B3LYP/6-31G and B3LYP/6-31G* are in good agreement with previously reported experimental values of polyglutamic acid and polylysine. Agreement with experiment improves when polarization functions are included in the basis set. Explicit water molecules, H-bonded to the backbone amide groups were found to be absolutely necessary to obtain this agreement. Our results indicate that DFT is a promising tool for assignment of the spectral data on kinetics of conformational changes for peptides during amyloid formation.

Keywords Polyglutamic acid · Assignment of Raman spectra · Density function theory · Conformational transition · Amide vibrational band · Peptide conformational change

W. M. Berhanu
NanoScience Technology Center and Department of Chemistry, University of Central Florida, Orlando, FL 32826, USA

I. A. Mikhailov
NanoScience Technology Center, University of Central Florida, Orlando, FL 32826, USA

A. E. Masunov (✉)
NanoScience Technology Center, Department of Chemistry, and Department of Physics, University of Central Florida, Orlando, FL 32826, USA
e-mail: amasunov@mail.ucf.edu

Introduction

Most neurodegenerative diseases, including Alzheimer's disease, are closely linked with accumulation and aggregation of the amyloid β-peptide (Aβ) produced through endoproteolysis of the β-amyloid precursor transmembrane protein. Experimental data also suggest that the neurotoxicity in these fatal diseases may be caused by the growing amyloid fibrils as well as soluble oligomers associated with them [1]. Formation of amyloid aggregates includes a conformational transition from alpha-helix into beta-sheet structure. Recent studies have revealed that amyloid formation is not a unique structural feature of a particular protein. On the contrary, any protein, under suitable conditions, can lose its native α-helical structure and aggregate [2, 3]. It has been well established that amyloid formation requires an appropriate physicochemical environment [2, 4]. However, the detailed mechanism of oligomer formation and the influence of protein stability on aggregation kinetics are still matters of debate. In order to study the dynamics of amyloid formation, different experimental techniques can be used. These include infrared (IR) and fluorescence spectroscopy [5–7], circular dichroism (CD) [8, 9], Raman optical activity (ROA) [10–13], Raman [14], and UV resonance Raman spectroscopy (UVRR) [11, 15–17].

Hydrogen bonding (H-bonding) is, in general, one of the most important determinants of alpha-helices, amyloids, and three-dimensional protein structure. The peptide units of the various residues engage in extensive hydrogen bonding with one another. They also interact with water molecules, which are found both within the protein and on its periphery. Hydration effects on peptide H-bonding must be understood in order to compare the stability of protein

conformations. Both intra-molecular protein–protein interactions and protein–solvent interactions determine native protein secondary and tertiary structures [18]. For example, intra-molecular protein hydrogen bonding stabilizes α-helical and β-sheet conformations [10, 19, 20], while protein–water interactions stabilize peptide and protein PPII conformations [21–23]. However, even though intra-molecular hydrogen bonding is expected to dominate for α-helical peptides, the solvation-shell water still may H-bond to the exposed N-H···O=C linkages that are intra-molecularly bonded [20, 24, 25]. Such interactions may also be important in the stabilization of the α-helix conformation [6, 26]. These hydrogen bonding interactions are expected to depend upon the extent to which the peptide side chain shields the peptide backbone from water.

The transition between α- and β-conformations is often believed to pass through a molten globe (or random coil) state with no conformational order. However, recent work by Asher et al. [16] has suggested that the alanine-based, mostly helical peptide AP melts from α-helical structure to a polyproline II (PPII)-type helix conformation. Such experimental evidence offers further support to theoretical studies that have suggested that small peptides in their unordered state (random coil) adopt a predominantly PPII helix conformation [17, 21–23, 27, 28]. This conformation was found to be unstable in gas phase, however. Adzhubei et al. [29] have suggested factors that they think are responsible for the stabilization of the PPII confirmation. According to these authors, H-bonding of the main chain with water molecules is the most probable stabilizing factor for PPII segments on the protein surface. H-bonds with water can also be formed by the side chains of these segments. There is mounting experimental evidence in favor of the PPII conformation in polypeptides being stabilized by water [30, 31]. This is supported also by free energy calculations and Monte-Carlo studies [32, 33]. These calculations show that the presence of solvent makes the PPII conformation energetically more favorable, in comparison with the conformation in vacuum [30]. Thus, hydration has a strong stabilizing effect on PPII-helices. Several forms of arrangement of water molecules around PPII segments have been observed [29].

Vibrational spectroscopic techniques such as Fourier transform infrared spectroscopy (FTIR) and Raman spectroscopy are generally considered to be low resolution techniques, which are useful solely for quantifying the contribution of distinct secondary structure motifs to the overall protein structure [34]. In this contribution, we will assess the ability of density functional theory (DFT) methods to predict Raman spectra with the accuracy necessary to detect conformational changes during amyloid formation. Raman spectroscopy is used to infer molecular structure and properties from vibrational transitions. It allows conformational changes to be detected [35]. In many aspects it is similar to IR spectroscopy, but has its own individual features. In contrast to IR, where radiation is absorbed by a sample, Raman experiments deal with radiation inelastically scattered by the molecule of interest.

The peptide bond itself has an absorption band in the UV region around 190 nm, so excitation of proteins and peptides with ~200 nm selectively enhances peptide backbone amide bands [36]. The resultant spectra are dominated by amide vibrations, designated as amide I, II, and III (Fig. 1) [34, 37]. Further, the spectrum carries easily recognizable features of different secondary structure elements. Using a library of proteins of known structure, Chi et al. [36] developed a methodology to correlate UV Raman spectral markers with the presence of secondary structure motifs. This methodology allowed the quantitative determination of the α-helix, β-sheet and random coil content of large proteins. H-bonding involving the C=O or N–H bonds and different elements of secondary structure affect bond strengths so that the amide I and amide II wavelengths are sensitive to the secondary structure content of a protein.

In order to provide physically reasonable electronic energies and their derivatives for polypeptides, a computationally affordable yet accurate theoretical method is needed. Kohn–Sham density functional theory (KS-DFT), which in principle describes electron correlation exactly, has become the method of choice to describe large biomolecules. Its efficiency is close to that of Hartree-Fock calculations and can be further enhanced by using density-fitting techniques when pure density functionals are employed [38]. Much of the previous work on Raman and ROA spectra have been done at the restricted Hartree-Fock (RHF) level of theory for the geometry and force field as well as for the polarizability tensors, and the solvent effect (water) was not taken into account. Deng et al. [39] predicted the Raman and ROA spectra of nine conformations of N-acetyl-L-alanine-N′-methylamide (AAMA) at the RHF/6-31G* level of theory. They did not, however, include any solvent effects in their calculations, and did not include polarization functions in the basis set. Han et al. [40] used the 6-311+G** basis set for the electric dipole electric dipole polarizability derivatives (EDEDPD), and the 6-31G* basis set for the electric dipole

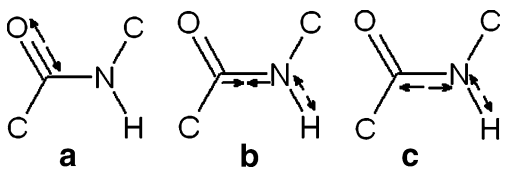

Fig. 1a–c Major contribution to normal modes corresponding to the atomic motion of amide bands. **a** Amide I mode is mostly carbonyl stretching vibration. **b** Amide II mode is an out-of-phase combination of C–N and N–H bond stretch. **c** Amide III mode is an in-phase combination of C–N and N–H bond stretch (adapted from [34, 37])

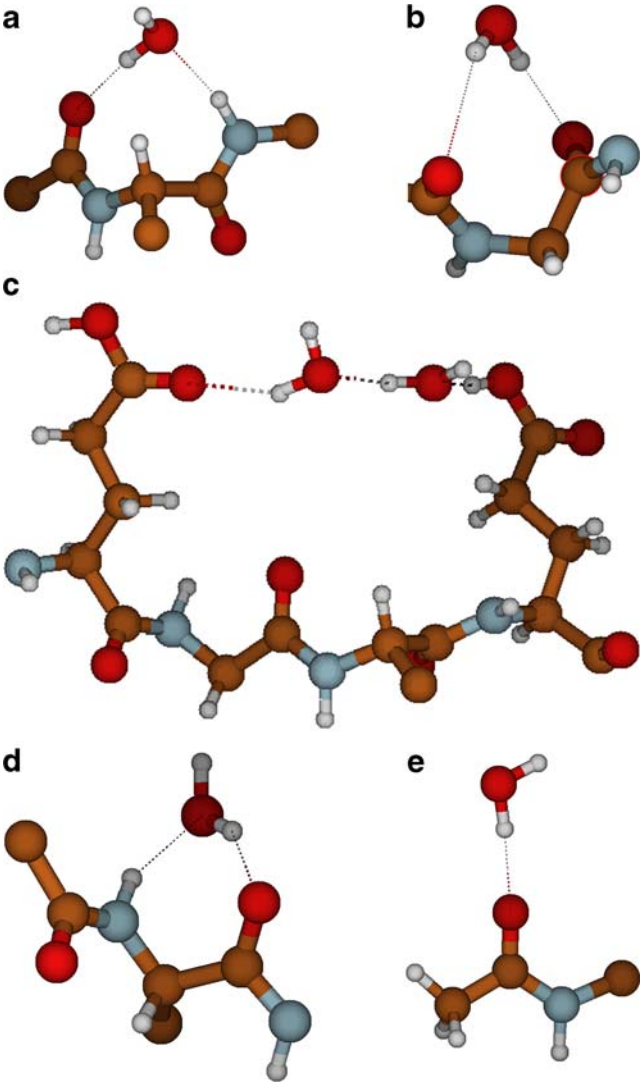

Fig. 2a–e Different hydrogen (H)-bonding modes of water molecules. **a** Water molecule bridging the amide and carbonyl group of consecutive amino acids residues. **b** Water molecule bridging the carbonyl groups of consecutive amino acids residues. **c** Water molecule bridging the carboxyl groups of the side chain of glutamic acids. **d** Water molecule bridging the amide and carbonyl groups of the same residue. **e** Water molecule forming a single H-bond to the CO group of the peptide backbone. *Broken lines* H-bonds

magnetic dipole polarizability derivatives (EDMDPD) and electric dipole electric quadrupole polarizability derivatives (EDEQPD) calculations. They extended previous studies by using the B3LYP level of theory, and also included water molecules, both explicitly and implicitly, in calculating the structures and atomic polar tensors (APT). By comparing calculated and observed Raman, vibrational circular dichroism (VCD), and ROA spectra, they suggested that the PPII structure of AAMA is the dominant one in aqueous solution.

Few other DFT studies on polypeptides had been published to date. Vaden et al. [41] characterized the inherent conformational preferences of the capped hexapeptide Ac-VQIVYK-NHMe in the gas phase. IR/UV double-resonance spectroscopy of the peptide isolated in a cold molecular beam was used to probe the conformation of the neutral peptide. The influence of protonation at the lysine side chain was investigated at 298 K by characterizing the protonated peptide ion, Ac-VQIVYK(H+)-NHMe, with infrared multiple-photon dissociation (IRMPD) spectroscopy in the fingerprint and amide I/II band region in an Fourier-transform ion cyclotron resonance (FTICR) mass spectrometer. The conformations for both neutral and protonated peptides were predicted by an extensive conformational search procedure followed by cluster analysis and then DFT calculations. Comparison of the experimental and computed IR spectra, with consideration of the relative energies, was used to assign the dominant conformations observed. The neutral peptide adopts a β-hairpin-like conformation with two loosely extended peptide chains, demonstrating the preference of the sequence for extended β-strand-like structures. In the protonated peptide, the lysine NH_3^+ disrupts this extended conformation by binding to the backbone and induces a transition to a random-coil-like structure.

The goal of this contribution was to test the accuracy of DFT method in predicting the conformational stability and Raman spectra of polypeptides in different conformations. We selected polyglutamic acid and polylysine as well defined systems for which reliable experimental data are

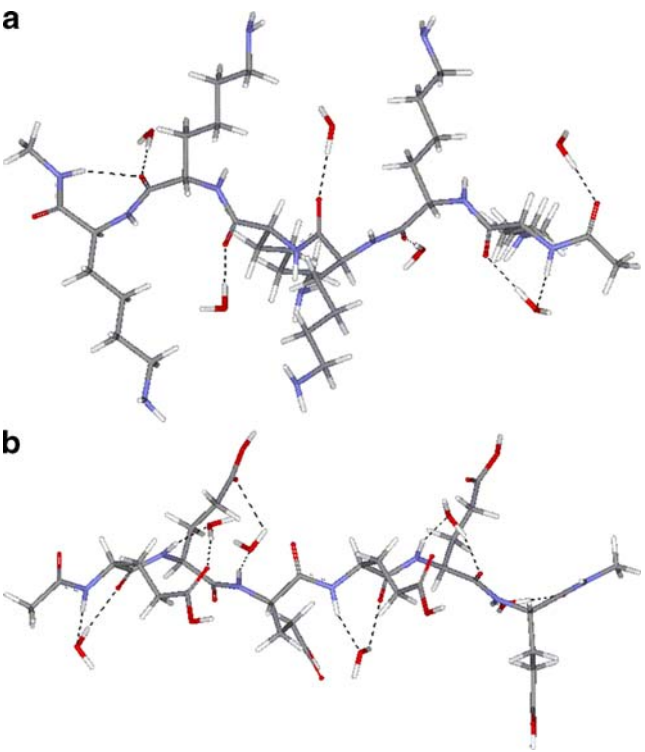

Fig. 3 Optimized geometry of the polyproline II (PPII) conformation of (**a**) lysine and (**b**) glutamic acid hexapeptides with water molecule H-bonding to the peptide backbone

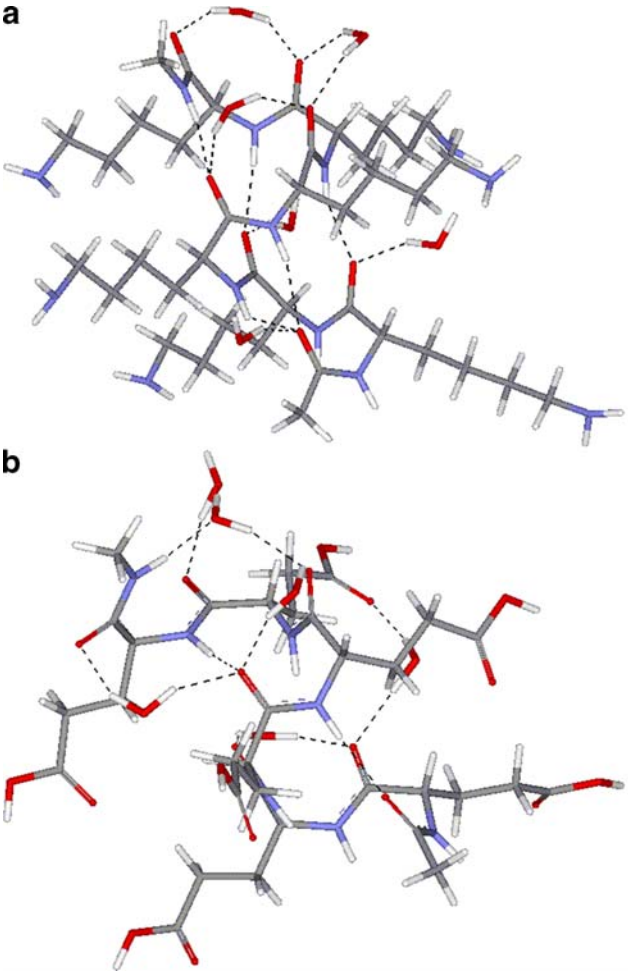

Fig. 4 Optimized geometry of alpha helix conformation of lysine hexapeptide (**a**) and glutamic acid (**b**) with water molecule H-bonding to the peptide backbone

available [35, 42]. To the best of our knowledge, this is the first DFT study of polyglutamic acid and polylysine. In this contribution we will assess the ability of DFT methods to predict Raman spectra with the accuracy necessary to detect conformational changes during amyloid formation. We compare the experimentally available Raman vibrational spectra with our calculations.

Computational details

All calculations used the Gaussian 2003 program [43]. Geometry optimizations and frequency calculations were carried out at the hybrid DFT level in the gas phase, using 6-31G and 6-31G* basis sets and B3LYP functional. The visualization and assignment of the vibrational modes was completed using the Molden program package [44, 45].

We studied three conformations of glutamic acid and lysine hexapeptides: (1) α-helix, (2) β-strand, and (3) "random coil" (PPII confirmation) [42]. The initial geometries of α-helix and β- strand conformations were obtained by modification of the respective conformations of the polyalanine [46]. The PPII confirmation was obtained by modification of the polyproline II fragment extracted from the Protein Data Bank (PDB structure with refcode 1AWI). The terminal amino and carboxylic groups were end-capped using acetyl and dimethylamine groups. Explicit water molecules were taken into account (one molecule per residue) for a total of six water molecules for one hexapeptide. The water molecules used in our calculations were not deuterated.

Results and discussion

Geometry optimization

When explicit water was not included in the system, the geometry optimization of the PPII conformation resulted in significant conformational change. This is in agreement with earlier report [29] that PPII does not present an energy minimum. In order to stabilize the PPII conformation we added six water molecules, H-bonded to the peptide. Four types of H-bonding patterns, found in X-ray structures containing PPII [29] were tested and are shown in Fig. 2. Each water molecule was used to bridge CO and NH

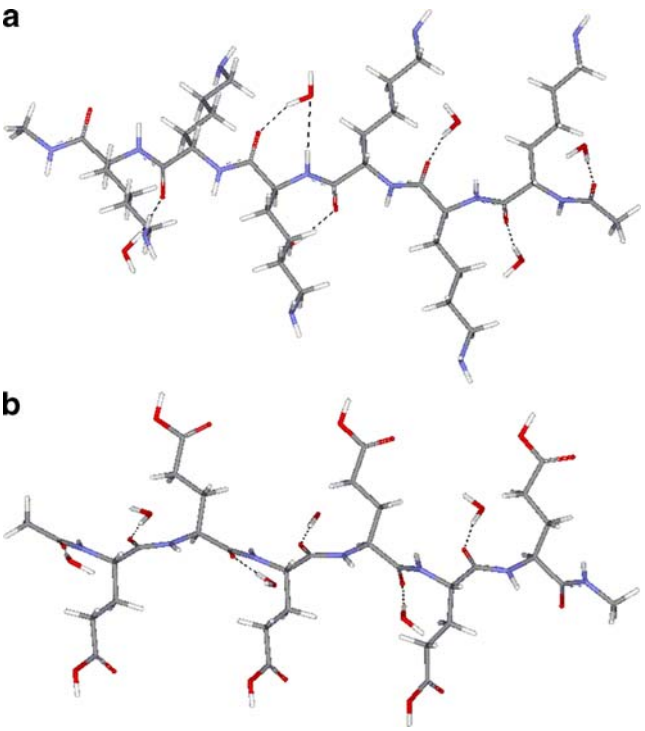

Fig. 5 Optimized geometry of beta sheet conformation of (**a**) lysine and (**b**) glutamic acid hexapeptides with water molecule H-bonding to the peptide backbone

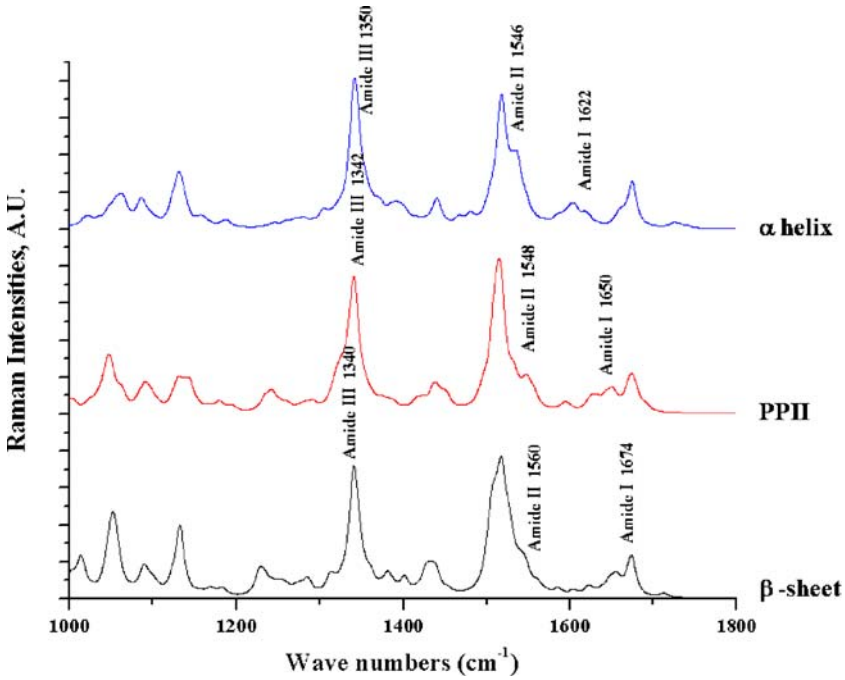

Fig. 6 Raman spectra of the α-helix, PPII, and β-sheet conformations of lysine hexapeptide, calculated at B3LYP/6-31G* theory level

groups of consecutive (Fig. 2a, b) or the same (Fig. 2d) residue(s). Alternatively, we tested bridging the carboxylic groups of the side chains (Fig. 2c) for the 1,3-residues, as well as water molecules H-bonded to one carbonyl group only (Fig. 2e). We found that the PPII conformation was retained only when water molecules H-bonded to NH and CO groups in the backbone of consecutive residues (Fig. 2a). The molecular structure of the optimized geometry of the PPII conformation of the lysine and glutamic acid hexapeptides are shown in Fig. 3.

The alpha helix and beta strand conformations were initially optimized in the gas phase. Next, these conformations were microsolvated with six water molecules. The configuration in which each water was bridging two carbonyl groups of the backbone was found to be the most stable and used thereafter to build hydrated alpha-helices.

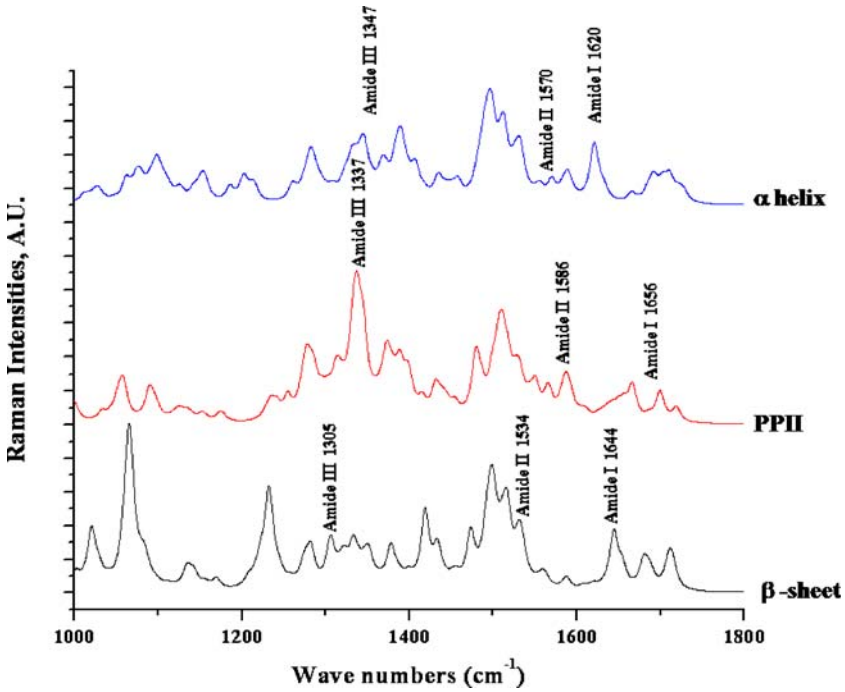

Fig. 7 Raman spectra of the α-helix, PPII, and β-sheet conformations of glutamic acid hexapeptide, calculated at B3LYP/6-31G* theory level

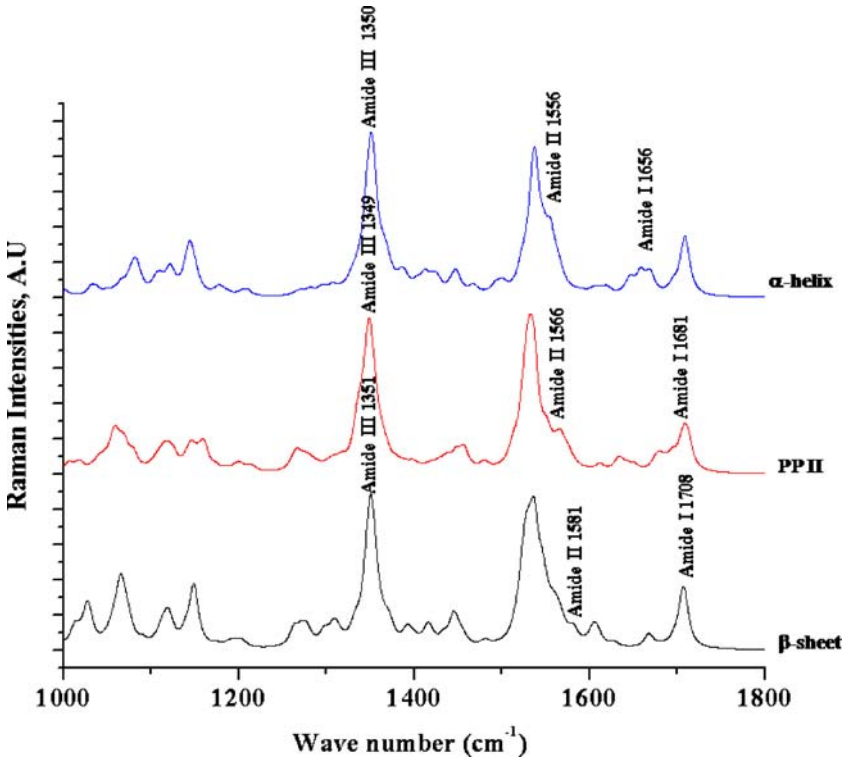

Fig. 8 Raman spectra of the α-helix, PPII, and β-sheet conformations of lysine hexapeptide, calculated at B3LYP/6-31G theory level

The optimized geometry of alpha helical lysine and glutamic acid hexapeptides are shown in Fig. 4. In the case of the beta strand, when one water molecule was used to bridge either NH and CO or two CO groups of the consecutive residues, this significantly altered the conformation. The only configuration stabilizing beta strands included a $CO\cdots H_2O\cdots HC_\alpha$ bridge with a non-classical hydrogen bond of the $CH\cdots O$ type and a length of ca. 2.8 Å. A similar type of hydrogen bonding were reported by Scheiner [45, and references therein], based on NMR spectra and first principle

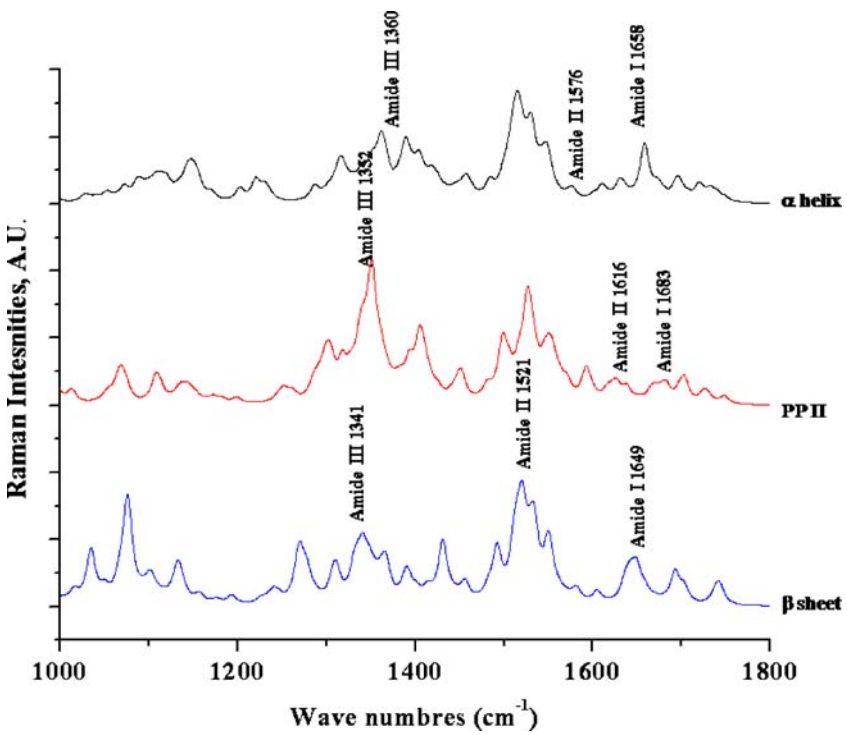

Fig. 9 Raman spectra of the α-helix, PPII, and β-sheet conformations of glutamic acid hexapeptide, calculated at B3LYP/6-31G theory level

Table 1 Amide I, II and III vibrational frequencies (in cm^{-1}) calculated for alpha helix and beta strand conformation of lysine hexapeptide in the gas phase, and the corresponding experimental values for polylysine in water (taken from [42])

Conformation	Theory level	Amide I	Amide II	Amide III
Alpha helix	B3LYP/6-31G	1,769	1,611	1,401
	B3LYP/6-31G*	1,726	1,582	1,382
	Experimental	1,644	1,548	1,275
Beta strand	B3LYP/6-31G	1,649	1,550	1,369
	B3LYP/6-31G*	1,632	1,550	1,356
	Experimental	1,661	1,559	1,244

simulations. The resulting configurations are shown in Fig. 5. The geometries optimized at B3LYP/6-31G and B3LYP/6-31G* were not visibly different, so only the latter are reported in all figures.

Raman spectra

The optimized geometries described above were used to predict Raman spectra for the lysine and glutamic acid hexapeptides. Figures 6, 7, 8, and 9 represent the spectra in the range between 1,000 and 1,800 cm^{-1}. The vibrational modes of interest are amide I, II, and III (defined in Fig. 1) are labeled on Figs. 6, 7, 8, and 9 along with their frequencies at the maximum. Other peaks of comparable intensity were observed close to amide I bands in the case of the glutamic acid hexapeptide. These correspond to vibrations of the COOH groups in the side chains.

The amide frequencies calculated for the gas phase are compared with experimental values in Tables 1 and 2. In the case of the beta strand conformations of lysine hexapeptide (Table 1), the frequencies for amide I and II are close to the experimental values. The predicted amide III for the isolated molecules is considerably larger (by about 120 cm^{-1}). The experimental value reported for amide I is 1661 for the beta sheet of polylysine in water, and the calculated values for the isolated lysine hexapeptide at B3LYP/6-31G and B3LYP/6-31G* are 1,649 and 1,932 cm^{-1} respectively. The beta strand conformations of glutamic acid hexapeptide (Table 2) and the frequencies for amide II vibrational modes obtained for the isolated molecules were close to the experimental values recorded in aqueous solution. The amide I predicted at 6-31G* (1,650 cm^{-1}) is very close to the experimental value of 1,648 and the prediction at 6-31G is found to be larger by 50 cm^{-1}.

For the α-helix conformations, the amide group is involved in the H-bond to the backbone carbonyl group. In the gas phase all NH groups of the backbone participate in H-bond already in the isolated molecule. Nonetheless, in the absence of explicit water molecules, larger frequencies for the amide I, II and III vibrational modes compared to the experimental values are predicted at both theory levels, as shown in Table 1. The disagreement with experimental values is especially large for amide I in the α-helix conformation of lysine hexapeptide. At B3LYP/6-31G level we predict it to be 1,769 cm^{-1}, which is about 120 cm^{-1} higher than the experimental value. The use of a larger basis set somewhat improves the value for amide I to 1,726 cm^{-1}, which is still larger by about 80 cm^{-1} than the experimental value. The values for amide I, II and III calculated at the B3LYP/6-31G* level are somewhat lower (and closer to experimental values), than those calculated at the B3LYP/6-31G level (see Table 1). The amide I calculated at B3LYP/6-31G for the α-helix conformation of the isolated glutamic acid hexapeptide is 1,688, which is about 30 cm^{-1} higher than the experimental value (Table 2). When the calculation was done at B3LYP/6-31G* in gas phase the value for amide I is 1,640, i.e., very close to 1,651 cm^{-1}—the experimental value for polyglutamic acids in aqueous solution.

Next, we will discuss the effect of microsolvation on the calculated Raman spectra. Table 3 shows the results of our calculations for the α-helix, PPII and beta strand conformations of the lysine hexapeptide with explicit water.

Table 2 Amide I, II and III vibrational frequencies (in cm^{-1}) calculated for alpha helix and beta strand conformation of the glutamic acid hexapeptide in gas phase and the experimental values for polyglutamic acid in water (taken from [42])

Conformation	Theory level	Amide I	Amide II	Amide III
Alpha helix	B3LYP/6-31G	1,688	1,553	1,374
	B3LYP/6-31G*	1,640	1,558	1,407
	Experimental	1,651	1,552	1,279
Beta strand	B3LYP/6-31G	1,702	1,545	1,361
	B3LYP/6-31G*	1,650	1,556	1,406
	Experimental	1,648	1,548	1,248

Table 3 Amide I, II and III vibrational frequencies (in cm^{-1}) calculated for three conformations of the lysine hexapeptide in the presence of explicit water molecules and the corresponding experimental values for polylysine in water (taken from [42])

Conformation	Theory level	Amide I	Amide II	Amide III
Alpha helix	B3LYP/6-31G	1,656	1,556	1,350
	B3LYP/6-31G*	1,622	1,546	1,369
	Experimental	1,644	1,548	1,275
Beta strand	B3LYP/6-31G	1,708	1,581	1,351
	B3LYP/6-31G*	1,674	1,560	1,340
	Experimental	1,661	1,559	1,244
PPII	B3LYP/6-31G	1,681	1,566	1,349
	B3LYP/6-31G*	1,650	1,548	1,342
	Experimental	1,655	1,559	1,258

Table 3 indicates that the DFT calculations for amide I and II for all three conformations of the lysine hexapeptide with explicit solvents using the 6-31G basis set overestimate the frequencies for amide normal modes compared to experimentally observed values in all cases, with maximal deviation of 47 cm^{-1}. When the calculation was performed with the 6-31G* basis set, the deviation from the experimental values was not more than 25 cm^{-1}. However, the calculated amide III vibrational frequencies with both 6-31G and 6-31G* basis sets are overestimated by about 100 cm^{-1} when compared to experimental values. The calculated amide III vibrational frequencies are 1,351 cm^{-1} and 1,340 cm^{-1} at the 6-31G and 6-31G* basis sets, respectively, and the experimental values for amide III was reported as 1,244 cm^{-1}. Figures 6 and 7 show the calculated spectra of lysine hexapeptide with explicit water at the 6-31G and 6-31G* basis sets, respectively.

Table 4 shows the result of calculations for the α-helix, beta strand, and PPII conformation of glutamic acid hexapeptides with explicit water. As one can see from Table 4, DFT predictions of the amide vibrational frequencies for glutamic acid hexapeptides are also in good agreement with experimental values. Again, the results obtained with the 6-31G basis set are overestimated in comparison with experimentally observed values, while calculations made using the 6-31G* basis set underestimate the frequency of amide I mode for all three conformations. The calculated amide III vibration frequency with both 6-31G and 6-31G* basis set are 1,341 cm^{-1} and 1,305 cm^{-1} and the corresponding experimentally reported value was 1,248 cm^{-1}. The DFT method again overestimated the amide III vibrational frequency, as in the case of lysine hexapeptides. The Raman spectra of the glutamic acid hexapeptides in the presence of explicit six water molecules calculated with 6-31G and 6-31G* basis sets are shown in Figs. 8 and 9 respectively.

Conclusions

We report the results of geometry optimization and predictions of Raman vibrational spectra using DFT for glutamic acid and lysine hexapeptides in three different conformations: PPII, beta strand and alpha helix, microsolvated with one water molecule per residue. When the solvent molecule is H-bonded to the backbone, B3LYP/6-31G* level of theory predicts Raman frequencies in good agreement with experimental values for amide I and II (ca. 25 cm^{-1} maximal deviation), while the accuracy for amide III vibrational frequencies is somewhat lower (within 100 cm^{-1}). All amide vibrational frequencies are overestimated when the 6-31G basis set was used. Based on these observations, we conclude

Table 4 Amide I, II and III vibrational frequencies (in cm^{-1}) calculated for three conformations of the glutamic acid hexapeptide in the presence of explicit water molecules and the corresponding experimental values for polyglutamic acid in water (taken from [42])

Conformation	Theory level	Amide I	Amide II	Amides III
Alpha helix	B3LYP/6-31G	1,658	1,576	1,360
	B3LYP/6-31G*	1,620	1,570	1,347
	Experimental	1,651	1,552	1,279
Beta strand	B3LYP/6-31G	1,649	1,521	1,341
	B3LYP/6-31G*	1,644	1,534	1,305
	Experimental	1,648	1,548	1,248
PPII	B3LYP/6-31G	1,683	1,616	1,352
	B3LYP/6-31G*	1,656	1,586	1,337
	Experimental	1,664	1,564	1,257

that DFT methods are capable of distinguishing vibrational spectra from different conformations of polypeptides [35]. Our calculations indicate that DFT methods can assist in assignment of spectral data recorded to detect observed conformational transitions of peptides, in particular during amyloid formation.

Acknowledgments This work was supported in part by the National Science Foundation (CCF/CHE 0832622). The authors are thankful to University of Central Florida (UCF) Institute for Simulations and Training (IST) HPC Stokes facility, UCF I2Lab, and the US Department of Energy National Energy Research Scientific Computing Center (DOE NERSC) for the generous donation of computer time. The authors would like to thank Prof. Alfonse Schulte for fruitful discussions.

References

1. Stefani M (2004) Biochim Biophys Acta 1739:5–25
2. Chiti F, Webster P, Taddei N, Clark A, Stefani M, Ramponi G, Dobson CM (1999) Proc Natl Acad Sci USA 96:3590–3594
3. Dobson CM (2001) Philos Trans R Soc Lond B 356:133–145
4. Fandrich M, Fletcher MA, Dobson CM (2001) Nature 410:165–166
5. Jas GS, Eaton WA, Hofrichter J (2001) J Phys Chem B 105:261–272
6. Manas ES, Getahun Z, Wright WW, DeGrado WF, Vanderkooi JM (2000) J Am Chem Soc 122:9883–9890
7. Maji SK, Amsden JJ, Rothschild KJ, Condron MM, Teplow DB (2005) Biochemistry 44:13365–13376
8. Fasman GD (1996) Circular dichroism and the conformational analaysis of biomolecules. Plenum, New York
9. Ozdemir A, Lednev IK, Asher SA (2002) Biochemistry 41:1893–1896
10. McColl IH, Blanch EW, Hecht L, Barron LD (2004) J Am Chem Soc 126:8181–8188
11. Barron LD, Hecht L, Ford SJ, Bell AF, Wilson G (1995) J Mol Struct 349:397–400
12. McColl IH, Blanch EW, Hecht L, Kallenbach NR, Barron LD (2004) J Am Chem Soc 126:5076–5077
13. Zhu FJ, Isaacs NW, Hecht L, Barron LD (2005) Structure 13:1409–1419
14. Spiro T (1987) Biological application of Raman spectroscopy, Vol 1. Raman spectra and the conformation of biological macromolecules. Wiley, New York
15. Chi ZH, Asher SA (1998) J Phys Chem B 102:9595–9602
16. Asher SA, Mikhonin AV, Bykov S (2004) J Am Chem Soc 126:8433–8440
17. Lednev IK, Karnoup AS, Sparrow MC, Asher SA (1999) J Am Chem Soc 121:8074–8086
18. Scheiner S, Kern CW (1977) J Am Chem Soc 99:7042–7050
19. Creighton TE (1993) Proteins: structures and molecular properties. Freeman, New York
20. Baker EN, Hubbard RE (1984) Prog Biophys Mol Biol 44:97–179
21. Bochicchio B, Tamburro AM (2002) Chirality 14:782–792
22. Martino M, Bavoso A, Guantieri V, Coviello A, Tamburro AM (2000) J Mol Struct 519:173–189
23. Mezei M, Fleming PJ, Srinivasan R, Rose GD (2004) Proteins 55:502–507
24. Gnanakaran S, Hochstrasser RM, Garcia AE (2004) Proc Natl Acad Sci USA 101:9229–9234
25. Thanki N, Thornton JM, Goodfellow JM (1988) J Mol Biol 202:637–657
26. Daggett V, Levitt M (1992) J Mol Biol 223:1121–1138
27. Stapley BJ, Creamer TP (1999) Protein Sci 8:587–595
28. Kelly MA, Chellgren BW, Rucker AL, Troutman JM, Fried MG, Miller AF, Creamer TP (2001) Biochemistry 40:14376–14383
29. Adzhubei AA, Sternberg MJE (1993) J Mol Biol 229:472–493
30. Makarov AA, Lobachov VM, Adzhubei IA, Esipova NG (1992) FEBS Lett 306:63–65
31. Makarov AA, Esipova NG, Lobachov VM, Grishkovsky BA, Pankov YA (1984) Biopolymers 23:5–22
32. Hodes ZI, Nemethy G, Scheraga HA (1979) Biopolymers 18:1565–1610
33. Eisenhaber F, Adjhubei AA, Eisenmenger F, Esipova NG (1992) Biofizika 37:62–67
34. Schweitzer-Stenner R (2006) Vib Spectrosc 42:98–117
35. Nielsen OF (2005) In: Jiskoot WCDJA (ed) Methods for structural analysis of protein pharmaceuticals. AAPS, Arlington, pp 167–199
36. Chi ZH, Chen XG, Holtz JSW, Asher SA (1998) Biochemistry 37:2854–2864
37. Diem M (1993) Introduction to modern vibrational spectroscopy. Wiley, New York
38. Herrmann C, Reiher M (2007) First-principles approach to vibrational spectroscopy of biomolecules. In: Reiher M (ed) Atomistic approaches in modern biology: from quantum chemistry to molecular simulations. Springer, Berlin, pp 85–132
39. Deng Z, Polavarapu PL, Ford SJ, Hecht L, Barron LD, Ewig CS, Jalkanen K (1996) J Phys Chem 100:2025–2034
40. Han WG, Jalkanen KJ, Elstner M, Suhai S (1998) J Phys Chem B 102:2587–2602
41. Vaden TD, Gowers SAN, de Boer T, Steill JD, Oomens J, Snoek LC (2008) J Am Chem Soc 130:14640–14650
42. Song SH, Asher SA (1989) J Am Chem Soc 111:4295–4305
43. Frisch MJ, Trucks GW, Schlegel HB, Scuseria GE, Robb MA, Cheeseman JR, Montgomery JA Jr, Vreven T, Kudin KN, Burant JC, Millam JM, Iyengar SS, Tomasi J, Barone V, Mennucci B, Cossi M, Scalmani G, Rega N, Petersson GA, Nakatsuji H, Hada M, Ehara M, Toyota K, Fukuda R, Hasegawa J, Ishida M, Nakajima T, Honda Y, Kitao O, Nakai H, Klene M, Li X, Knox JE, Hratchian HP, Cross JB, Bakken V, Adamo C, Jaramillo J, Gomperts R, Stratmann RE, Yazyev O, Austin AJ, Cammi R, Pomelli C, Ochterski JW, Ayala PY, Morokuma K, Voth GA, Salvador P, Dannenberg JJ, Zakrzewski VG, Dapprich S, Daniels AD, Strain MC, Farkas O, Malick DK, Rabuck AD, Raghavachari K, Foresman JB, Ortiz JV, Cui Q, Baboul AG, Clifford S, Cioslowski J, Stefanov BB, Liu G, Liashenko A, Piskorz P, Komaromi I, Martin RL, Fox DJ, Keith T, Al-Laham MA, Peng CY, Nanayakkara A, Challacombe M, Gill PMW, Johnson B, Chen W, Wong MW, Gonzalez C, Pople JA (2004) Gaussian 03, Rev E.01. Gaussian Inc, Wallingford CT
44. Noordik GSJH (2000) J Comput Aided Mol Des 14:123–134
45. Scheiner S (2009) J Phys Chem B 113:10421–10427
46. Wieczorek R, Dannenberg JJ (2004) J Am Chem Soc 126:14198–14205